Journal of Power Sources 265 (2014) 291–298

Contents lists available at ScienceDirect

Journal of Power Sources

journal homepage: www.elsevier.com/locate/jpowsour

Bivariate quadratic method in quantifying the differential capacitance and energy capacity of supercapacitors under high current operation

Chin-Teng Goh*, Andrew Cruden

Energy Technology Group, Engineering Sciences, University of Southampton, Highfield, Southampton SO17 1BJ, UK

HIGHLIGHTS

- A bivariate quadratic method for the electrical characteristics of supercapacitors.
- The capacitance and energy capacity are derived directly from terminal measurements.
- The capacitance–voltage characteristic is more complex than a linear function.
- The capacitance exhibits variation between charging and discharging states.
- Up to 79% of the total energy is available within the 50%–100% nominal voltage range.

ARTICLE INFO

Article history:
Received 9 December 2013
Received in revised form
19 April 2014
Accepted 28 April 2014
Available online 9 May 2014

Keywords:
Supercapacitor
Bivariate quadratic
Differential capacitance
Voltage dependent
Constant current charging discharging
Energy capacity

ABSTRACT

Capacitance and resistance are the fundamental electrical parameters used to evaluate the electrical characteristics of a supercapacitor, namely the dynamic voltage response, energy capacity, state of charge and health condition. In the British Standards EN62391 and EN62576, the constant capacitance method can be further improved with a differential capacitance that more accurately describes the dynamic voltage response of supercapacitors. This paper presents a novel bivariate quadratic based method to model the dynamic voltage response of supercapacitors under high current charge–discharge cycling, and to enable the derivation of the differential capacitance and energy capacity directly from terminal measurements, i.e. voltage and current, rather than from multiple pulsed-current or excitation signal tests across different bias levels. The estimation results the author achieves are in close agreement with experimental measurements, within a relative error of 0.2%, at various high current levels (25–200 A), more accurate than the constant capacitance method (4–7%). The archival value of this paper is the introduction of an improved quantification method for the electrical characteristics of supercapacitors, and the disclosure of the distinct properties of supercapacitors: the nonlinear capacitance–voltage characteristic, capacitance variation between charging and discharging, and distribution of energy capacity across the operating voltage window.

1. Introduction

In the electrical modelling of supercapacitors, capacitance and resistance are the fundamental electrical parameters used to evaluate the electrical characteristics of a supercapacitor, namely the dynamic voltage response, energy capacity, energy loss, state of charge and health condition. The capacitance of supercapacitors (electrochemical capacitors) consists of two main charge storage principles: double-layer capacitance and pseudocapacitance [1,2], depending on the electrode material used. In double-layer capacitance, charge is stored electrostatically in the interface between an electrode and an electrolyte. When an external voltage is applied on one electrode, the counter-ions of the electrolyte are attracted to the surface of the electrode, forming two layers of charge that separated by a molecular dielectric layer (mono-layer of solvent molecules) at the electrode–electrolyte interface. In pseudocapacitance, the storage mechanism is a reversible Faradaic charge-transfer process, achieved by the adhesion of electrolyte ions onto the surface of electrode (made up of metal oxides or conducting polymers) via electrosorption, intercalation or reduction–oxidation reactions.

The capacitance of a supercapacitor is susceptible to changes in operating conditions such as voltage, frequency, temperature, and charge propagation [3–5], mainly related to the mobility of charge

* Corresponding author. Tel.: +44 02380593242; fax: +44 02380593016.
E-mail addresses: c.goh@soton.ac.uk, gohchinteng@gmail.com (C.-T. Goh).

http://dx.doi.org/10.1016/j.jpowsour.2014.04.139
0378-7753/

during operation. The voltage dependency of the device capacitance can be explained by the effect of the applied electric field on the permittivity of the molecular dielectric, the separation of the charge layer and the molarity of electrolyte. Besides, the capacitance is proportional to the effective area of the charge layer that formed at the electrode–electrolyte interface during operation, not the total surface area of typically highly porous electrode. This effective area depends on the accessibility of electrode pores and the propagation of electrolyte ions into the different pore depths/sizes of electrode. The propagation of ions takes longer time to reach long narrow pores than short wide pores, hence resulting in higher capacitance (due to larger effective area) at lower frequency operation. This explains both the charge and frequency effects on the capacitance.

In the British Standards EN62391 [6] and EN62576 [7] (identical to IEC62391 and IEC62576), the capacitance of supercapacitors is quantified as a constant capacitance by using the constant current discharge test method, without considering the voltage and charge dependencies of the supercapacitor. This constant capacitance based identification method is found to be inadequate to precisely represent the dynamic terminal behaviour of supercapacitors [8–10].

The term differential capacitance is the measurement of capacitance as a function of voltage. Differential capacitance is commonly introduced within the electrical models of supercapacitor to describe the voltage dependency of capacitance. In the deployment of differential capacitance in various resistor–capacitor equivalent circuit models, the main challenge is obviously to accurately establish the relationship of capacitance versus voltage, which can be identified from either the frequency response to a small excitation signal (typically currents of a few mA), e.g. in tests using electrochemical impedance spectroscopy (EIS) [4,11], or the voltage response to a controlled pulse-current (in tens of Amperes) in studies using the constant current test method [12–14] repeatedly across different bias levels. The differential capacitance can then be modelled as a linear function [4,12,14–16], a quadratic function [11], or even a quartic function [17]. The order of function relates to the size of the experimental dataset (number of bias levels) used in defining the relationship of capacitance versus voltage. Studies with small datasets consume less experimental time and generally allow simple analysis compared to studies with large datasets; however the precision of modelling could be comprised.

Apart from the linear capacitance–voltage based equivalent circuit models, several analytical models have been proposed to model the dynamic behaviour of supercapacitors. These models are ladder network model with a complex pore impedance block [18], transmission line model with the hybridisation of temporal and frequency approaches [11], artificial neural network based models [19–21], and fractional non-linear model [22]. In these models, the parameters identification often involves intensive experimentation and computation to achieve good approximation results.

This paper presents a highly accurate and practical method to model the dynamic voltage response, and quantify the differential capacitance and energy capacity of supercapacitors under high current operations (up to 200 A) that typically experienced in real-life applications. A bivariate quadratic function is developed and applied for the first time to represent the dynamic charge–voltage characteristic of supercapacitors. This proposed method allows the differential capacitance and energy capacity of supercapacitors to be derived directly from the terminal measurements, i.e. voltage and current, rather than from multiple pulse-current or excitation signal tests at different bias levels as discussed previously. Hence, the bivariate quadratic based method can eliminate the trade-off between accuracy and practicality (i.e. simplicity of testing) in identifying the capacitance–voltage characteristic for the electrical modelling of supercapacitors.

2. Experimental

This study aims to understand the dynamic behaviour of supercapacitors during the high power/current operations often experienced in real-life applications. In the laboratory, these operating conditions are recreated as constant current charging–discharging experiments by using a programmable high current test system. The high current test system [10] developed by the authors, supports three types of charge/discharge/cycling current profile – constant current, sinusoidal current, and customised current cycles, at current levels up to 250 A. A data acquisition device, based on a National Instrument USB-6218, is deployed to record the voltage, current and temperature measurements of the supercapacitor under test.

High current charging–discharging experiments were conducted on Maxwell's Boostcap supercapacitors. The specifications of these double-layer based supercapacitors are an equivalent series resistance (ESR) of 0.8 mΩ, a nominal capacitance of 650 F, and a rated voltage of 2.7 V. From a constant current charging–discharging experiment of 200 A, the voltage response of a 650 F supercapacitor cell operated between 0 and 2.7 V is as depicted in Fig. 1. The current signal is the effective square wave, with a corresponding triangular voltage response. The 'charge' currents are represented by negative values whilst the 'discharge' currents are represented by positive values. Both the voltage and current time series data are subsequently used as the input data for the proposed numerical method, described in following section.

3. Bivariate quadratic method

3.1. Simple resistor–capacitor circuit

For practical purposes, a simple series resistor–capacitor (RC) equivalent circuit is applied to represent the dynamic voltage response of supercapacitors during fast charging–discharging. The circuit parameters are stated as the equivalent series resistance (ESR) and differential capacitance, as shown in Fig. 2. In terms of circuit notation, the terminal voltage of the supercapacitor is denoted as V_{SC}, the current of the supercapacitor as I_{SC}, the voltage across the ESR as V_R, and the differential capacitor voltage is V_C.

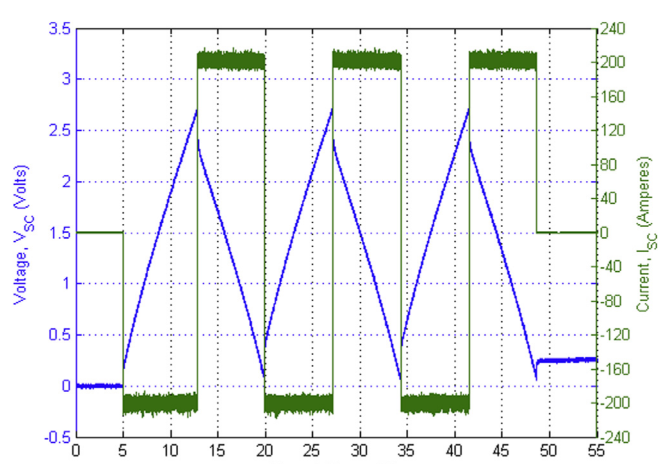

Fig. 1. The voltage response of a supercapacitor under charge–discharge cycling at 200 A.

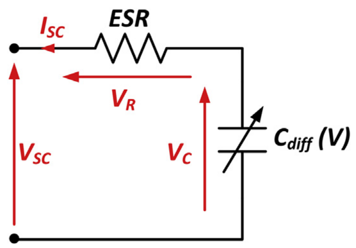

Fig. 2. Simple RC equivalent circuit of a supercapacitor.

Within the context of this paper, the "capacitor" term refers to the differential capacitance, not the entire supercapacitor cell.

3.1.1. Equivalent series resistance

The voltage–time characteristic of a supercapacitor during a constant current charging–discharging cycle is illustrated in Fig. 3. The ESR parameter can be identified from the abrupt voltage change (rise or fall) at the start or end of the charging or discharging state. This abrupt voltage change is due to the change in voltage across the ESR, V_R, when there is a step change in current, ΔI_{SC}.

$$\mathrm{ESR} = \frac{V_R}{\Delta I_{SC}} \tag{1}$$

From Figs. 1 and 3, the abrupt voltage change at the start of the discharging state (time t_2) is twice the level at the start of charging (time t_1) due to a twofold increase in the step change in current ($\Delta I_{SC} = 2 \times I_{SC}$). Thus, the ESR determined at times t_1 and t_2 should be close in value to each other. V_{min} and V_{max} are the minimum and maximum voltage points defined during the constant current cycling experiment.

3.1.2. Differential capacitance

A linear capacitor, by definition, exhibits a linear increase in voltage, V, with respect to charge, Q, implying its capacitance, C, is always constant.

$$C = \frac{Q}{V} = \frac{dQ}{dV} \tag{2}$$

A supercapacitor (a form of non-linear capacitor) exhibits a differential increase in voltage, V', with respect to charge, Q. The differential capacitance, C_{diff}, is obtained from:

$$C_{diff} = \frac{dQ}{dV'} \tag{3}$$

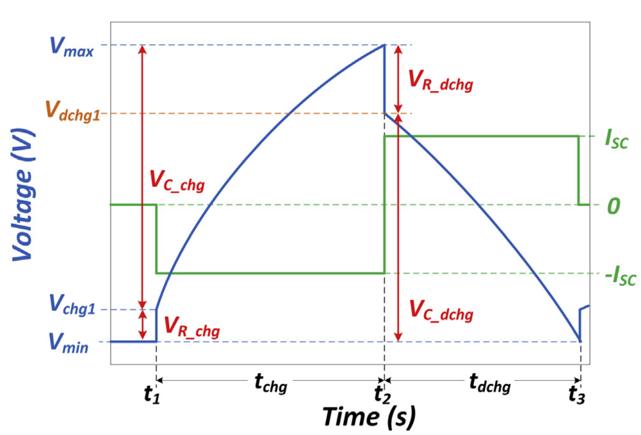

Fig. 3. The voltage–time characteristic of a supercapacitor under constant current cycling.

By referring to (3), the differential capacitance of a supercapacitor can be determined from the derivative of its charge–voltage characteristic. In order to establish the relationship of voltage versus charge, the charge exchanged during the experiment is calculated by using the measured current time series data. At a constant current I_{SC}, the charge exchanged during charging (between t_1 and t_2), Q_{chg}, and charge exchanged during discharging (between t_2 and t_3), Q_{dchg}, are determined from:

$$Q_{chg} = \int_{t_1}^{t_2} I_{SC} dt \tag{4}$$

$$Q_{dchg} = \int_{t_2}^{t_3} I_{SC} dt \tag{5}$$

3.2. Bivariate quadratic equation

By considering the voltage and charge dependencies of the capacitance, the authors propose a new bivariate quadratic based method to approximate the charge–voltage characteristic of a supercapacitor. The derivative and integral of the proposed approximation are used to quantify the differential capacitance and energy capacity properties of the supercapacitor respectively. The bivariate quadratic equation is therefore of the following form:

$$Ax^2 + Bxy + Cy^2 + Dx + Ey = 1 \tag{6}$$

where x relates to charge, Q, y relates to voltage, V, and the coefficients, A to E, require to be determined.

The proposed approximation, developed with the Matlab® numerical computing environment, comprises four simple steps to accurately represent the charge–voltage characteristic of a supercapacitor. The procedures are as follows:

3.2.1. Step 1: select five data points

With five unknown coefficients in Equation (6), five data points, Pt1 to Pt5, are required to be chosen from the charge–voltage characteristic so that these points are equally spaced along the charge, Q, axis, as shown in Fig. 4.

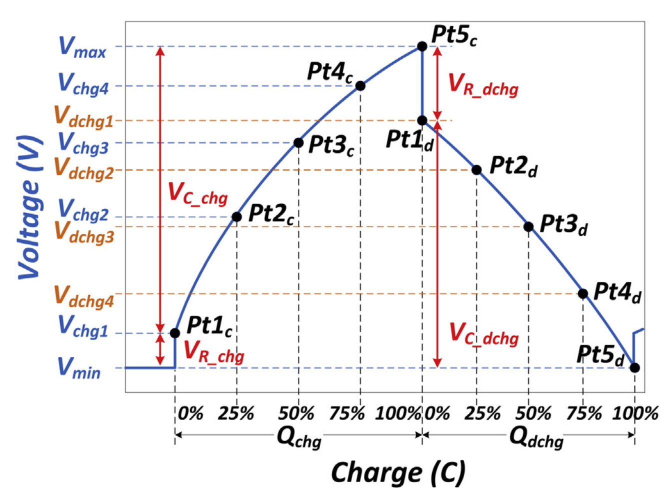

Fig. 4. The charge–voltage characteristic of supercapacitor under constant current cycling.

3.2.2. Step 2: translate coordinate plane

Numerical computation on the five unknown coefficients of A to E could result in unlimited possible values, hence in order to simplify the computation process, the charge–voltage plane (Q–V plane) is translated into the x–y plane so that the two data points of Pt1 and Pt5 intersect at the new horizontal, x, and vertical, y, axes respectively.

During the charging state, the translating equations are:

$$x = Q - Q_{\mathrm{chg}} \tag{7}$$

$$y = V - V_{\mathrm{chg1}} \tag{8}$$

During the discharging state, the translating equations are:

$$x = Q \tag{9}$$

$$y = V - V_{\mathrm{min}} \tag{10}$$

3.2.3. Step 3: determine the coefficients (A to E) of the bivariate quadratic equation

By substituting the translated data points (in x–y plane) into Equation (6), the resulting equations can be written in the matrix form as follow:

$$\begin{bmatrix} x_1^2 & x_1y_1 & y_1^2 & x_1 & y_1 \\ x_2^2 & x_2y_2 & y_2^2 & x_2 & y_2 \\ x_3^2 & x_3y_3 & y_3^2 & x_3 & y_3 \\ x_4^2 & x_4y_4 & y_4^2 & x_4 & y_4 \\ x_5^2 & x_5y_5 & y_5^2 & x_5 & y_5 \end{bmatrix} \cdot \begin{bmatrix} A \\ B \\ C \\ D \\ E \end{bmatrix} = \begin{bmatrix} 1 \\ 1 \\ 1 \\ 1 \\ 1 \end{bmatrix} \tag{11}$$

The coefficients of A to E can be determined by using the matrix inversion method.

$$\begin{bmatrix} A \\ B \\ C \\ D \\ E \end{bmatrix} = \begin{bmatrix} x_1^2 & x_1y_1 & y_1^2 & x_1 & y_1 \\ x_2^2 & x_2y_2 & y_2^2 & x_2 & y_2 \\ x_3^2 & x_3y_3 & y_3^2 & x_3 & y_3 \\ x_4^2 & x_4y_4 & y_4^2 & x_4 & y_4 \\ x_5^2 & x_5y_5 & y_5^2 & x_5 & y_5 \end{bmatrix}^{-1} \cdot \begin{bmatrix} 1 \\ 1 \\ 1 \\ 1 \\ 1 \end{bmatrix} \tag{12}$$

3.2.4. Step 4: approximate the charge–voltage characteristic of supercapacitors

For a quadratic function $f(y) = ay^2 + by + c$, its roots (values of y which $f(y) = 0$) are

$$y = \frac{-b \pm \sqrt{\Delta}}{2a} \tag{13}$$

where the discriminant, $\Delta = b^2 - 4ac$.

Once the coefficients of A to E are identified, the approximation of the voltage response of the supercapacitor with respect to charge is computed according to the root-finding method described in Equation (13).

Re-arranging Equation (6) given:

$$y^2 + \left(\frac{Bx + E}{C}\right)y + \frac{Ax^2 + Dx - 1}{C} = 0 \tag{14}$$

The roots of Equation (14) are:

$$y = \frac{1}{2}\left(-\left(\frac{Bx+E}{C}\right) \pm \sqrt{\left(\frac{Bx+E}{C}\right)^2 - 4\left(\frac{Ax^2+Dx-1}{C}\right)}\right) \tag{15}$$

By substituting the translating Equations (7)–(11) into Equation (15), the charge–voltage characteristic of the supercapacitor is approximated by the following equations.

During the charging state:

$$V_{\mathrm{SC}}(Q) = \frac{1}{2}\left(-\left(\frac{Bx+E}{C}\right) \pm \sqrt{\left(\frac{Bx+E}{C}\right)^2 - 4\left(\frac{Ax^2+Dx-1}{C}\right)}\right) + V_{\mathrm{chg1}} \tag{16}$$

where $x = Q - Q_{\mathrm{chg}}$.

During the discharging state:

$$V_{\mathrm{SC}}(Q) = \frac{1}{2}\left(-\left(\frac{BQ+E}{C}\right) \pm \sqrt{\left(\frac{BQ+E}{C}\right)^2 - 4\left(\frac{AQ^2+DQ-1}{C}\right)}\right) + V_{\mathrm{min}} \tag{17}$$

Next, the derivative of x with respect to y ($\mathrm{d}x/\mathrm{d}y$) of the bivariate quadratic equation is determined via implicit differentiation.

$$\frac{\mathrm{d}x}{\mathrm{d}y} = -\frac{Bx + 2Cy + E}{2Ax + By + D} \tag{18}$$

As the translation from the Q–V coordinate plane to the x–y coordinate plane has no effect on the gradient of the polynomial, the differential capacitance C_{diff} in Equation (3) can be written as:

$$C_{\mathrm{diff}} = \frac{\mathrm{d}Q}{\mathrm{d}V'} = \frac{\mathrm{d}x}{\mathrm{d}y} \tag{19}$$

During the charging state:

$$C_{\mathrm{diff\_chg}} = -\frac{B\left(Q - Q_{\mathrm{chg}}\right) + 2C\left(V - V_{\mathrm{chg1}}\right) + E}{2A\left(Q - Q_{\mathrm{chg}}\right) + B\left(V - V_{\mathrm{chg1}}\right) + D} \tag{20}$$

During the discharging state:

$$C_{\mathrm{diff\_dchg}} = -\frac{BQ + 2C(V - V_{\mathrm{min}}) + E}{2AQ + B(V - V_{\mathrm{min}}) + D} \tag{21}$$

3.3. Energy capacity of a supercapacitor

At a constant charge current I_{SC}, the amount of energy a supercapacitor exchanged (stored in charging state and released in discharging state) can be determined by calculating the area under the charge–voltage curve, as shown in Fig. 5. The energy dissipated in the ESR is denoted as E_R, the energy exchanged in the differential capacitor is denoted as E_C, also known as capacitor energy, and the energy remaining inside the capacitor before the charging or after the discharging is denoted as E_{Re}. The E_{Re} is only applicable to those experiments with a non-zero minimum voltage (or end voltage), V_{min}.

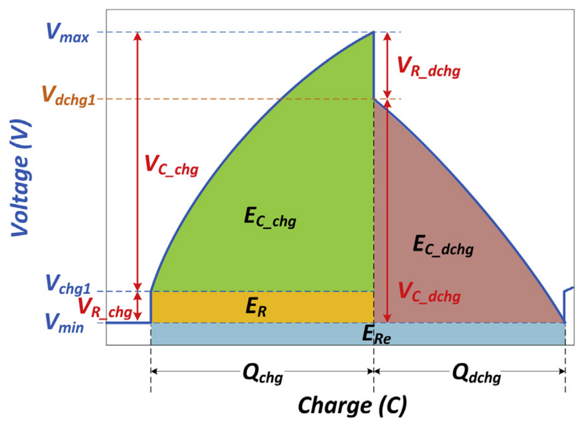

Fig. 5. The energy components of supercapacitor under constant current charging–discharging.

The quantification of capacitor energy is achieved by applying the trapezium rule. By discretising the area under the charge–voltage curve into N equally spaced panels, the capacitor energy is quantified as follows:

During the charging state, the dissipated energy in ESR, E_R:

$$E_R = V_{R\_chg} \times Q_{chg} \tag{22}$$

The capacitor energy, E_C:

$$E_{C\_chg} \approx h\left(\frac{1}{2}(V_{SC}(Q_1)+V_{SC}(Q_{N+1}))+\sum_{k=2}^{N}V_{SC}(Q_k)\right)-V_{chg1}\times Q_{chg} \tag{23}$$

where spacing, $h = Q_{chg}/N$ and $V_{SC}(Q)$ was defined in Equation (16).

During the discharging state, the remaining energy inside the capacitor, E_{Re}:

$$E_{Re} = V_{min} \times Q_{dchg} \tag{24}$$

The capacitor energy, E_C:

$$E_{C\_dchg} \approx h\left(\frac{1}{2}(V_{SC}(Q_1)+V_{SC}(Q_{N+1}))+\sum_{k=2}^{N}V_{SC}(Q_k)\right)-V_{min}\times Q_{dchg} \tag{25}$$

where spacing, $h = Q_{dchg}/N$ and $V_{SC}(Q)$ was defined in Equation (17).

3.3.1. Energy equivalent capacitance

For comparative reasons discussed later, the following energy equivalent linear capacitance is now defined. At a given capacitor voltage V_C, the energy equivalent capacitance, C_E, of a linear capacitor storing the same amount of energy as the differential capacitance of the supercapacitor is given as:

$$C_E = \frac{2E_C}{V_C^2} \tag{26}$$

4. Results and discussion

In this section, the modelling accuracy of the proposed bivariate quadratic method in representing the dynamic voltage response of supercapacitors under high current charging–discharging is evaluated and compared with the constant capacitance method. The quantification of differential capacitance and energy capacity (capacitor energy) which have been derived directly from the terminal measurements, are presented and discussed.

4.1. Experimental results

The electrical characteristics of 650 F Maxwell Boostcap supercapacitors were evaluated using constant current charge–discharge experiments at current levels of 25 A, 50 A, 100 A and 200 A. In these experiments, the initially uncharged supercapacitors were cycled between a minimum voltage of 0 V and a maximum voltage of 2.7 V. At the end of each cycle, the lowest achievable voltage level was limited to 0.06 V due to the tolerance in the voltage sensing circuit of the high current test system. The following discussion is based on a ‘fresh’, i.e. new, 650 F Maxwell Boostcap supercapacitor (labelled as E22), which has an ESR of 0.8 mΩ and a nominal capacitance of 650 F.

The voltage response of the supercapacitor E22 during the first cycle of the constant current experiment of 25 A is shown in Fig. 6. An abrupt voltage change of 0.012 V responding to a step change in current of 24.9 A is recorded at the start of charging state whilst an abrupt voltage change of 0.05 V responding to a step change in current of 52.8 A is recorded at the start of discharging state. The resultant ESR is computed to be 0.47 mΩ in the charging state whilst 0.95 mΩ in the discharging state. These computed ESR values are close to the specified ESR of 0.8 mΩ. During the charging state, the measurements of exchanged charge, internally dissipated energy and capacitor energy are 1694.6 C, 20.0 J and 2449.6 J respectively. During the discharging state, the measurements of exchanged charge, remaining energy (due to non-zero end voltage) and capacitor energy are 1617.6 C, 207.9 J and 2124.8 J respectively. Similar measurements were obtained from constant current cycling experiments carried out at 50 A and 200 A, and were then compiled and shown in Table 1.

By referring to the experimental results in Table 1, the ESR was found to be between 0.5 mΩ and 1.0 mΩ, close to the specified value of 0.8 mΩ. This indicates that the supercapacitor E22 is in pristine condition. Next observation is that an increase in operating current level results an increase in the dissipated energy, E_R, and a decrease in the exchanged charge, Q, and capacitor energy, E_C, of the supercapacitor. This can be attributed to the increase in the voltage drop across the ESR that reduces the effective working voltage window of the supercapacitor. Next, the remaining energy, E_{Re}, at the end of the constant current cycle is caused by the lowest

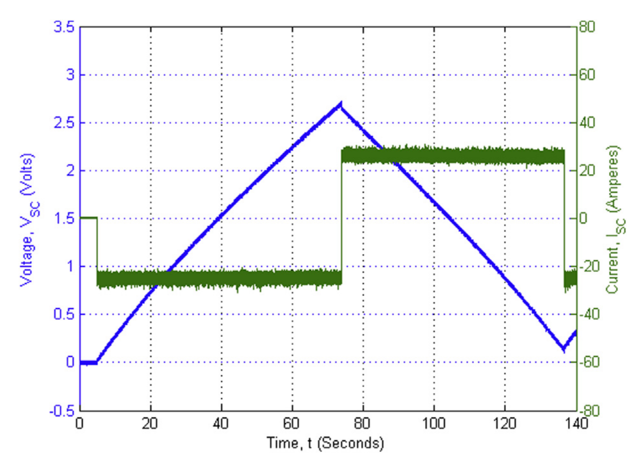

Fig. 6. The terminal response of supercapacitor E22 during the first cycle of 25 A cycling experiment.

Table 1
Experimental results (first cycle) of supercapacitor E22 at different current levels.

Current I_{SC} (A)	Charging state				Discharging state			
	ESR (mΩ)	Q_{chg} (C)	E_R (J)	E_{C_chg} (J)	ESR (mΩ)	Q_{dchg} (C)	E_{Re} (J)	E_{C_dchg} (J)
25	0.47	1694.6	20.0	2449.6	0.95	1617.6	207.9	2124.8
50	0.52	1663.7	43.2	2368.0	0.94	1596.9	95.8	2102.1
100	0.68	1639.6	112.7	2303.7	1.03	1532.3	107.3	1942.7
200	0.69	1574.0	220.4	2175.4	0.92	1426.0	92.7	1695.1

voltage level of 0.06 V that can be achieved by the high current test system. In the 25 A experiment, the E_{Re} is twofold the values recorded in 50–200 A experiments due to the recorded end voltage of 0.129 V.

4.2. Charge–voltage characteristic

By applying the procedures described in Section. 3.2, a bivariate quadratic equation was developed from five experimental data points to represent the charge–voltage characteristic of supercapacitor E22. In Figs. 7 and 8, the charge–voltage characteristic during 25 A charging and discharging are shown, together with the approximation results based on the constant capacitance method and the bivariate quadratic method. The experimental data is plotted is blue (in the web version); the constant capacitance approximation is plotted in green; and the proposed bivariate quadratic approximation is plotted in red. In both figures, the experimental data is closely represented by the author's proposed model compared to the conventional constant capacitance method. The gradient of the estimated charge–voltage curve is assessed to quantify the differential capacitance of supercapacitor E22 in Section. 4.3. Another observation is that the charging phase charge–voltage curve exhibits larger variation in the gradient than the discharging phase charge–voltage curve.

4.3. Differential capacitance

The differential capacitance of supercapacitor E22 is identified from the derivative of the bivariate quadratic equation, i.e. Equations (20) and (21). The voltage dependency of this capacitance at current levels of 25 A, 50 A, 100 A and 200 A is shown in Fig. 9, with the capacitance increasing with terminal voltage. The relationship of capacitance versus voltage is more complex than a linear function which is suggested in some characterisation studies. In the 25 A charging state, the capacitance is found to be 630.41 F using the constant capacitance method (Equation (2)) whilst in the range of 456 F–749 F using the author's proposed method. In the 25 A discharging state, the capacitance is 641.53 F with the constant capacitance method whilst in the range of 557 F–696 F with the proposed method. In addition to the voltage dependency of capacitance, the capacitance variation between charging and discharging states should be considered in electrical modelling of supercapacitors. By applying the differential capacitance identified from the proposed method, the dynamic voltage response of supercapacitor E22 is well predicted, as shown in Fig. 10.

4.4. Energy capacity

The energy capacity of supercapacitor E22 is assessed by measuring the amount of energy exchanged (stored or released) within the differential capacitance during the charging and discharging states. The energy–voltage characteristic during 25 A charging–discharging is shown in Fig. 11, together with the approximation results based on the constant capacitance method and the proposed bivariate quadratic method. In the 25 A cycling, the exchanged energy is measured as 2449.6 J during charging and 2124.8 J during discharging. In the charging state, the estimation of capacitor energy, E_C, and its accuracy with respect to the recorded result are 2277.8 J (92.99%) using the conventional constant capacitance method, whilst it is 2448.2 J (99.94%) using the author's bivariate quadratic method. In the discharging state, the estimation of capacitor energy and its accuracy with respect to the recorded result are 2039.4 J (95.98%) using the conventional constant capacitance method, whilst it is 2125.1 J (100.01%) using the author's bivariate quadratic method.

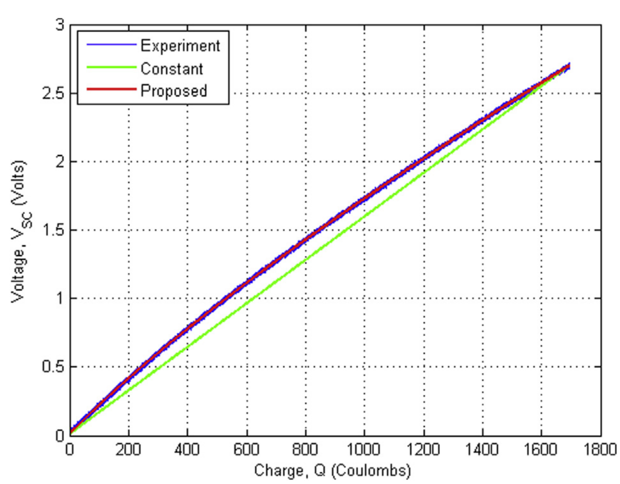

Fig. 7. The charge–voltage characteristic of supercapacitor E22 under 25 A charging.

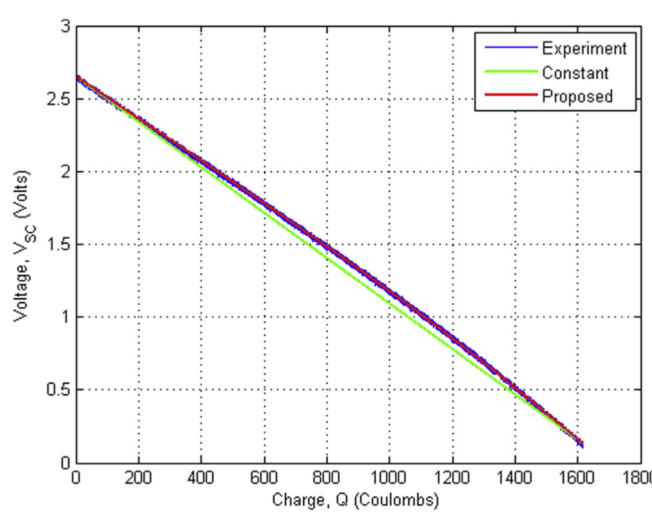

Fig. 8. The charge–voltage characteristic of supercapacitor E22 under 25 A discharging.

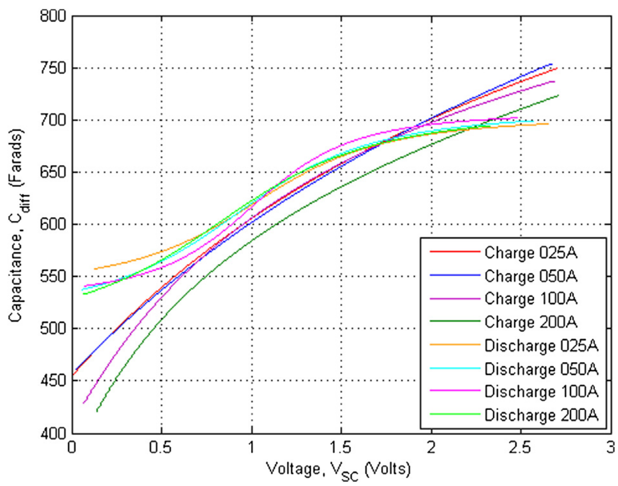

Fig. 9. The differential capacitance of supercapacitor E22 derived from the bivariate quadratic method at different current levels.

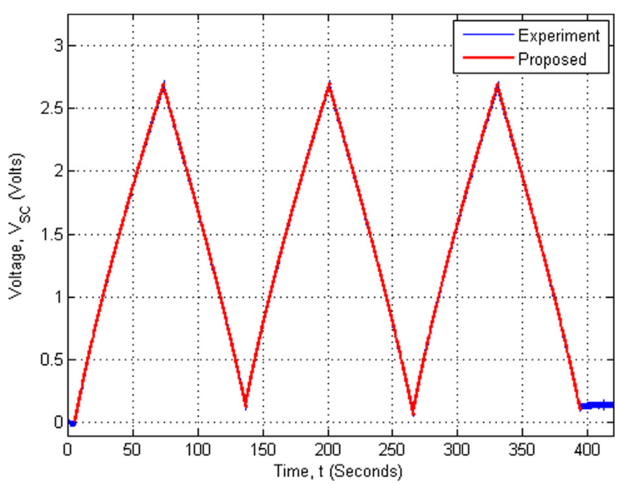

Fig. 10. The dynamic voltage response of supercapacitor E22 under 25 A cycling.

Table 2
The capacitor energy and energy equivalent capacitance of supercapacitor E22 at different current levels.

Current I_{SC} (A)	Actual E_C (J)	Constant capacitance		Bivariate quadratic	
		E_C (J)	C_E (F)	E_C (J)	C_E (F)
Charging					
25	2449.6	2277.8 (92.99%)	630.41	2448.2 (99.94%)	677.58
50	2368.0	2199.4 (92.88%)	629.21	2365.7 (99.90%)	676.80
100	2303.7	2143.2 (93.03%)	627.20	2304.6 (100.04%)	674.43
200	2175.4	2022.6 (92.97%)	612.44	2173.0 (99.89%)	658.00
Discharging					
25	2124.8	2039.4 (95.98%)	641.53	2125.1 (100.01%)	668.49
50	2102.1	2004.1 (95.34%)	636.23	2101.4 (99.97%)	667.12
100	1942.7	1846.4 (95.04%)	635.79	1941.9 (99.96%)	668.70
200	1695.1	1614.9 (95.27%)	629.57	1692.0 (99.82%)	659.64

Similar estimation results were obtained from constant current cycling experiments at 50 A, 100 A and 200 A, and then compiled and shown in Table 2. In terms of estimation accuracy, the proposed bivariate quadratic method achieves a relative error of just 0.2% compared to the actual measurements whilst the constant capacitance method has an error range of 4%–7%. The energy equivalent capacitance, C_E, is the capacitance of a linear capacitor that contains the same effective energy amount as the differential capacitance of supercapacitor. The C_E is around 678 F in the charging state whilst 668 F in the discharging state. These values are 104.2% and 102.8% respectively of the capacitance value stated on the nameplate of supercapacitor E22.

An accurate estimation of the supercapacitor energy capacity, which relates to the value of the differential capacitance, is particularly important for the estimation of the state of charge of supercapacitors. The energy capacity between the half rated voltage and the rated voltage is computed as 75% of the total energy, based on the constant capacitance method. However, practically this is not the case for supercapacitor E22 due to the influence of differential capacitance. By referring to the distribution of energy capacity plot in Fig. 12, approximately 79% of the device energy capacity is available between the half rated voltage and the rated voltage.

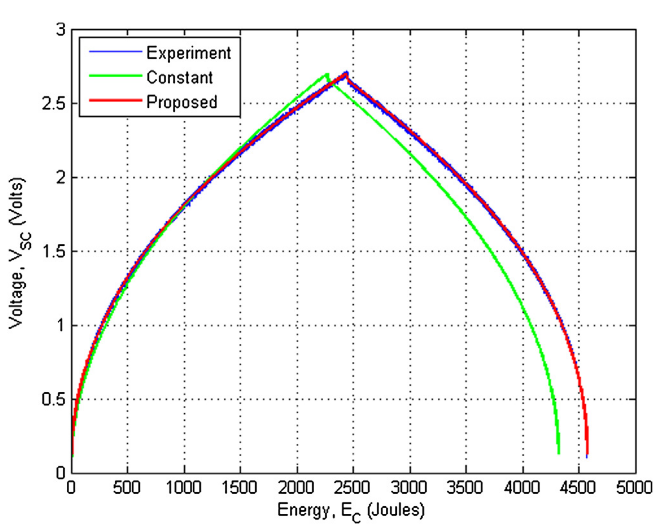

Fig. 11. The energy–voltage characteristic of supercapacitor E22 under 25 A charging–discharging.

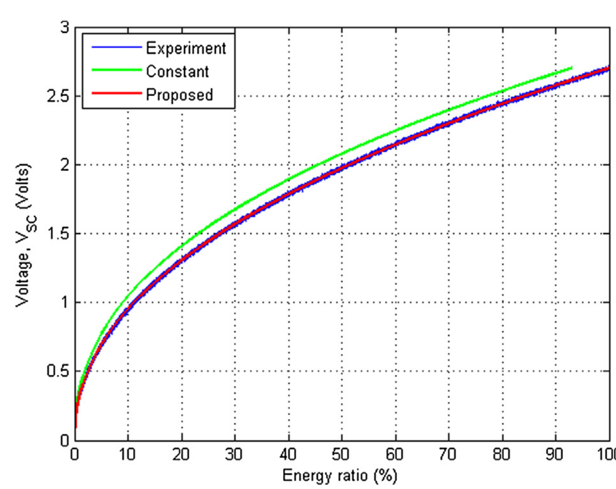

Fig. 12. The distribution of energy capacity in supercapacitor E22 under 25 A charging.

5. Conclusions

In this paper, the authors have developed a bivariate quadratic approximation method and applied it for the first time to represent the dynamic electrical behaviour of supercapacitors under constant current cycling across an operating current range of 25 A–200 A. This proposed method allows the differential capacitance and energy capacity of supercapacitors to be derived directly from the terminal measurements of voltage and current. This eliminates the need to establish the relationship of capacitance versus voltage from multiple pulsed-current or excitation signal tests at different bias levels [4,11–14]. The approximation results of the bivariate quadratic method are in close agreement with the experimental measurements at different current levels of 25 A–200 A. For the estimation of the capacitor energy, the relative error is 0.2% using the proposed method whilst in a range of 4%–7% using the constant capacitance method.

The quantification of differential capacitance and energy capacity leads to three important observations in the study of the electrical characteristics of supercapacitors. Firstly, the increase of capacitance with respect to voltage is more complex than a linear function. Secondly, the capacitance exhibits variation between charging and discharging states, and finally, approximately 79% of the energy capacity is available between the half rated voltage and the rated voltage, not 75% as typically understood. The proposed method therefore can achieve a more accurate electrical model of supercapacitors than the conventional constant capacitance method, and it is hoped that this new technique will be further adopted in the state of charge estimation of supercapacitors, with the aim to reduce the cumulative energy/state of charge error over repeated cycles. In practice, the proposed method can be implemented as an online diagnosis tool to analyse the health condition of supercapacitors with high accuracy, by using only the terminal measurements of voltage and current.

Acknowledgement

The authors gratefully acknowledge the financial support given to this work by the EPSRC under the SUPERGEN—The Energy Storage Consortium Program (EP/H019596/1), www.energy-storage.org.uk.

References

[1] B.E. Conway, Electrochemical Supercapacitors: Scientific Fundamentals and Technological Applications, Kluwer Academic/Plenum, New York, 1999.
[2] B.E. Conway, W.G. Pell, J. Solid State Electrochem. 7 (2003) 637–644.
[3] R. Kotz, M. Hahn, R. Gallay, J. Power Sources 154 (2006) 550–555.
[4] F. Rafik, H. Gualous, R. Gallay, A. Crausaz, A. Berthon, J. Power Sources 165 (2007) 928–934.
[5] J.W. Graydon, M. Panjehshahi, D.W. Kirk, J. Power Sources 245 (2014) 822–829.
[6] British_Standards, BS EN 62391-1, 2006, pp. 13–17.
[7] British_Standards, BS EN 62576, 2010, pp. 10–13.
[8] P. Mahon, G. Paul, S. Keshishian, A. Vassallo, J. Power Sources 91 (2000) 68–76.
[9] S. Buller, M. Thele, R.W.A.A. De Doncker, E. Karden, IEEE Trans. Ind. Appl. 41 (2005) 742–747.
[10] C.T. Goh, A. Cruden, in: 21st International Symposium on Power Electronics, Electrical Drives, Automation and Motion, SPEEDAM 2012, June 20, 2012–June 22, 2012, IEEE Computer Society, Sorrento, Italy, 2012, pp. 748–753.
[11] N. Rizoug, P. Bartholomeus, P. Le Moigne, IEEE Trans. Ind. Electron. 57 (2010) 3980–3990.
[12] L. Zubieta, R. Bonert, IEEE Trans. Ind. Appl. 36 (2000) 199–205.
[13] F. Belhachemi, S. Rael, B. Davat, in: 35th IAS Annual Meeting and World Conference on Industrial Applications of Electrical Energy, October 8, 2000–October 12, 2000, IEEE, Rome, Italy, 2000, pp. 3069–3076.
[14] R. Faranda, Electr. Power Syst. Res. 80 (2010) 363–371.
[15] W. Lajnef, J.M. Vinassa, O. Briat, S. Azzopardi, E. Woirgard, J. Power Sources 168 (2007) 553–560.
[16] A. Berrueta, I. San Martin, A. Hernandez, A. Ursua, P. Sanchis, J. Power Sources 259 (2014) 154–165.
[17] R.L. Spyker, R.M. Nelms, IEEE Trans. Aerosp. Electron. Syst. 36 (2000) 829–836.
[18] S. Buller, E. Karden, D. Kok, R. De Doncker, IEEE Trans. Ind. Appl. 38 (2002) 1622–1626.
[19] J.N. Marie-Francoise, H. Gualous, A. Berthon, IEEE Proc. Electr. Power Appl. 153 (2006) 255–262.
[20] A. Eddahech, O. Briat, M. Ayadi, J.-M. Vinassa, Electr. Power Syst. Res. 106 (2014) 134–141.
[21] C.H. Wu, Y.H. Hung, C.W. Hong, Energy Convers. Manage. 53 (2012) 337–345.
[22] N. Bertrand, J. Sabatier, O. Briat, J.-M. Vinassa, Commun. Nonlinear Sci. Numer. Simul. 15 (2010) 1327–1337.